A comparison of high-order and plane wave enriched boundary element basis functions for Helmholtz problems

B. Gilvey[1] and J. Trevelyan [*1]

[1]*Department of Engineering, Durham University, South Road, Durham DH1 3LE, UK*

October 14, 2020

Abstract

When undertaking a numerical solution of Helmholtz problems using the Boundary Element Method (BEM) it is common to employ low-order Lagrange polynomials, or more recently Non-Uniform Rational B-Splines (NURBS), as basis functions. A popular alternative for high frequency problems is to use an enriched basis, such as the plane wave basis used in the Partition of Unity Boundary Element Method (PUBEM). To the authors' knowledge there is yet to be a thorough quantification of the numerical error incurred as a result of employing high-order NURBS and Lagrange polynomials for wave-based problems in a BEM setting. This is the focus of the current work, along with comparison of the results against PUBEM. The results show expected improvements in the convergence rates of a Lagrange or NURBS scheme as the order of the basis functions is increased, with the NURBS basis slightly outperforming the Lagrange basis. High-order Lagrange and NURBS formulations can compare favourably against PUBEM for certain cases. In addition, the recently observed pollution effect in BEM is studied for a travelling wave in a duct and the numerical dispersion presented for all three sets of basis functions.

Keywords: BEM, PUBEM, high-order, pollution, isogeometric

1 Introduction

In solving wave problems engineers have a variety of numerical methods available. For high-frequency problems there are methods based on statistical energy descriptions or on physical optics. For lower frequencies where, for example, it may be important to capture diffraction effects, engineers typically rely on the discrete methods, the most popular of which are the Finite Element Method (FEM) and BEM, the latter of which is the focus of the current work. Further, without prejudice against the time-domain methods which are important for many classes of wave problem, our focus in this paper is the frequency-domain approach in which the waves are assumed to propagate at a single frequency. In this case the governing wave equation reduces to a time-harmonic form known as the Helmholtz equation. In approximating the solution to this equation, both the finite and boundary element methods are classically formulated by expressing the solution element-wise in the form of a piecewise polynomial variation. Thus, the problem is reduced to seeking the amplitudes of these polynomial basis functions.

There are different sources of error in these numerical methods. Firstly, the discretisation error, which results from the fact that the solution cannot generally be written as a set of (typically low-order) piecewise polynomial functions. Secondly, there may be integration errors in computing

---

[*]Corresponding author. E-mail: jon.trevelyan@durham.ac.uk

terms in the system matrices. And thirdly, it has been widely reported that the FEM suffers from the pollution effect [1, 2], which is manifested in a progressive error in capturing the wavelength over a long distance and can be described as a form of numerical dispersion. In order to control discretisation errors, one can adhere to certain heuristic rules; a common one suggests the use of 8-10 degrees of freedom per wavelength to capture what is essentially a sinusoidal solution. However, as the frequency increases, care is required since adhering to such a heuristic alone will become insufficient to control pollution errors.

In the search for more accurate and/or efficient approximations, researchers have investigated the use of different basis functions that might improve upon low-order piecewise polynomials. There have been a number of methods comprising high-order basis functions, including the use of Bernstein and Lobatto polynomials, which show promising results [3,4] and are further explored as the Bernstein-Bézier Finite Element Method (BBFEM) [5] (which also admits the use of static condensation to improve computational efficiency). Other improvements to FEM aimed at the high-frequency regime have been made by utilising the Partition of Unity Method [6,7] such as the Partition of Unity Finite Element Method (PUFEM) [8,9] and the Variational Theory of Complex Rays (VTCR) [10], in which plane waves are used to form the basis, therefore injecting the correct sinusoidal behaviour of the solution directly into the element formulation. A number of discontinuous plane-wave enrichment schemes have also been presented, such as the Plane Wave Discontinuous Galerkin Method (PWDG) [11, 12], the Discontinuous Enrichment Method [13], and the Ultraweak Variational Formulation (UWVF) [14], the latter of which has been shown to be a special case of PWDG. All of these so-called 'enriched' methods are inspired by Trefftz methods, since solutions to the governing PDE are used to inform the choice of basis.

Reformulating the governing PDE using Green's second identity produces a boundary integral equation, the discretisation of which forms the foundation of the BEM. This reduces the dimensionality of a given problem, meaning that instead of requiring the computation of volumetric integrals in $3D$, only surface integration is required, with $2D$ surface integrals becoming $1D$ line integrals. Whilst this reduction in dimensionality offers benefit for interior acoustic problems, the greatest improvements are found when considering exterior problems in an unbounded domain. Taking a scattering problem as an example, only the boundary of the scattering object would require discretisation, but acoustic variables could be recovered at any location as a result. In addition, by virtue of employing Green's functions which are free-space solutions to the governing PDE, the Sommerfeld radiation condition [15] (which states that nothing is reflected from infinity) is satisfied by construction. By contrast, a finite element model of a scattering problem requires an artificial domain truncation and some non-reflecting boundary condition prescribed over the truncation boundary. It is for these reasons that BEM presents an attractive alternative in particular for scattering problems.

Traditional BEM approaches employ similar techniques to describe the variation of the acoustic variable as FEM, i.e. piecewise polynomial Lagrangian shape functions. Trefftz-based methods can also be applied in order to obtain accurate solutions from coarse discretisations. A plane wave basis is used in the Partition of Unity BEM (PUBEM) [16–18] wherein it has been shown that the number of degrees of freedom per wavelength in each coordinate direction required to achieve 'engineering accuracy' may be reduced from $8 - 10$ to approximately 2.5. This is a general or engineering-type approach because the number of enrichment waves and their directions can be varied, allowing for solution of problems in a wide class of geometries, including those with reflections such as scattering from non-convex obstacles. This is noteworthy as there are more problem-specific enrichment methods wherein leading order behaviour is built-in to the enrichment [19,20] to obtain extremely efficient and accurate solutions for certain classes of problem. Another Trefftz boundary approach (though not BEM) is the Method of Fundamental Solutions (MFS) [21] which for many problems can give an attractive combination of accuracy and computational efficiency.

Isogeometric analysis (IGA) [22] is a numerical technique that employs a spline basis, such as NURBS, and has gained popularity in recent years. This is due to the fact that it allows direct importation of geometries from CAD, exact representation of geometries formed from conic sections,

and improved convergence properties afforded to it by its smooth, non-negative basis functions. Since its inception IGA has been developed for a number of applications [23–25], in a BEM setting (termed IGABEM) [26–28] and using T-splines for acoustics problems [29]. IGA lends itself well to BEM due to the fact that an IGABEM model can be obtained directly from CAD, whereas using FEM a volumetric NURBS description would be required, and this is non-trivial to generate from most CAD model boundary representations. The benefit of NURBS boundary discretisations has been combined with a plane wave basis [30, 31] to form the eXtended Isogeometric Boundary Element Method (XIBEM).

With such a broad spectrum of basis functions available, it is timely to compare their numerical performance. In a finite element context, high-order polynomial basis functions and wave-based methods have been compared [32] and another comparison made between BBFEM and PUFEM [5]. Recently, high-order finite element IGA (IGAFEM) schemes [33, 34] have been studied for acoustic problems, but with no comparison against the equivalent enriched scheme. To the authors' knowledge this has not been extended to a boundary element setting. Thus, the focus of this paper is as follows. Firstly, we explore the numerical performance of high-order basis functions for acoustics problems in BEM, namely NURBS and Lagrangian shape functions. Secondly, we compare the results with PUBEM in the form of L^2 error and condition number κ of the resulting system of equations. In addition, the existence of some pollution error in BEM has recently been demonstrated [35], and quantified for a number of low-order basis functions. Pollution error for high-order and enriched bases are investigated in the current work and illustrated through an example of a travelling wave propagating in a long duct. While it might be suggested that the inclusion of an analytical plane wave in the basis functions would eliminate pollution, the pollution effect has been observed in a PWDG setting [36] (apart from the trivial case in which the basis includes the pure direction of propagation of a single plane wave). To the authors' knowledge this has not been studied for a plane wave boundary element basis.

2 Boundary Integral Equation

2.1 Formulation

The Helmholtz equation and relevant boundary conditions are presented in this section, along with the corresponding Boundary Integral Equation (BIE). Both interior wave propagation and exterior scattering problems are considered in this paper, the latter of which requires the inclusion of an incident wave in the the BIE. For convenience in both the interior and exterior cases we define a domain contained by each geometry as $\Omega \subset R^2$ having boundary Γ. The domain containing the medium in which acoustic waves propagate is defined as $\Omega_f = R^2 \backslash \Omega$ for the external scattering problems and $\Omega_f = \Omega$ for the interior problem. We begin with the Helmholtz equation, which is the time-harmonic wave equation.

$$\nabla^2 \phi(\mathbf{x}) + k^2 \phi(\mathbf{x}) = 0, \quad \mathbf{x} \in \Omega_f \tag{1}$$

wherein ∇^2 is the Laplacian operator, k is the wave number which is defined as $k = 2\pi/\lambda$ (where λ is the wavelength under consideration) and the unknown acoustic potential is denoted as $\phi \in C$. Imposing a Robin boundary condition on (1), given by

$$\frac{\partial \phi(\mathbf{q})}{\partial \mathbf{n}} = \alpha \phi(\mathbf{q}) + \beta, \quad \mathbf{q} \in \Gamma \tag{2}$$

then employing Green's second identity [37] to reformulate the Helmholtz equation as a BIE in terms of 'source' and 'field' points ($\mathbf{p}$ and $\mathbf{q}$ respectively), which are located on the boundary Γ, provides

3

the following:

$$c(\mathbf{p})\phi(\mathbf{p}) + \int_{\Gamma}\left[\frac{\partial G(\mathbf{p},\mathbf{q})}{\partial \mathbf{n}} - \alpha G(\mathbf{p},\mathbf{q})\right]\phi(\mathbf{q})d\Gamma_{\mathbf{q}} = \int_{\Gamma}\beta G(\mathbf{p},\mathbf{q})d\Gamma_{\mathbf{q}} + \phi^{inc}(\mathbf{p}). \tag{3}$$

In the above, $c(\mathbf{p})$ is referred to as a 'jump' term and varies depending on the external angle of the boundary Γ at the locations of $\mathbf{p}$. ϕ^{inc} is an incident wave which is only to be included for exterior scattering problems and the vector $\mathbf{n}$ is the outward facing unit normal vector from Ω_f. A direct collocation method is employed, wherein (3) is satisfied at the chosen set of collocation points $\mathbf{p}$, instead of a Galerkin scheme, which would require multiplication of (3) by a test function and integrating over Γ. The Green's function for the Helmholtz equation in $2D$ is defined as follows,

$$G(\mathbf{p},\mathbf{q}) = \frac{i}{4}H_0^{(1)}(kr), \tag{4}$$

where $H_0^{(1)}$ is the Hankel function of the first kind and of order zero, and r is the Euclidian distance between $\mathbf{p}$ and $\mathbf{q}$. In order to solve (3) we discretise Γ into E elements, with S basis functions to describe the variation over an element e, to produce

$$c(\mathbf{p})\phi(\mathbf{p}) + \sum_{e=1}^{E}\sum_{s=1}^{S}\int_{-1}^{1}\left[\frac{\partial G(\mathbf{p},\mathbf{q})}{\partial \mathbf{n}} - \alpha G(\mathbf{p},\mathbf{q})\right]\Psi_s(\xi)J^e d\xi \phi_s^e = \int_{\Gamma}\beta G(\mathbf{p},\mathbf{q})d\Gamma_{\mathbf{q}} + \phi^{inc}(\mathbf{p}), \tag{5}$$

in which Ψ_s denotes the basis functions, which remain general at this stage, ϕ_s^e represent the unknowns describing the potential distribution, J^e is the Jacobian of the geometric mapping $(x,y) \to \xi$ and the local coordinate $\xi \in [-1,1]$ is employed over each element. This results in the following linear system of equations in matrix form.

$$\left[\mathbf{C} + \mathbf{H} - \boldsymbol{\alpha}\mathbf{G}\right]\left\{\boldsymbol{\phi}\right\} = \left\{\boldsymbol{\beta}\mathbf{b} + \boldsymbol{\phi}^{inc}\right\}, \tag{6}$$

where $\mathbf{C}$ contains the interpolations of $c(\mathbf{p})$, $\mathbf{H}$ and $\boldsymbol{\alpha}\mathbf{G}$ contain the boundary integrals from the left hand side of (5), ϕ is the vector of the unknowns, $\boldsymbol{\beta}\mathbf{b}$ is a vector containing the boundary integrals from the right hand side of (5) and $\boldsymbol{\phi}^{inc}$ is a vector of evaluations of the incident wave potential at the collocation locations. The order of the basis employed is equal to $S - 1$, thus $S = 3$ produces a quadratic basis, of order 2 and $S = 12$ produces a basis of order 11.

2.2   Basis functions

2.2.1   Lagrange polynomials.

The first basis functions considered are conventional Lagrangian shape functions, which describe ϕ as follows.

$$\phi = \sum_{s=1}^{S}\Psi_s^L(\xi)\phi_s^e, \tag{7}$$

where

$$\Psi_s^L(\xi) := \prod_{\substack{0 \le m \le S \\ m \ne s}}\frac{\xi - \xi_m}{\xi_s - \xi_m} = \frac{(\xi - \xi_0)}{(\xi_s - \xi_0)}\cdots\frac{(\xi - \xi_{s-1})}{(\xi_s - \xi_{s-1})}\frac{(\xi - \xi_{s+1})}{(\xi_s - \xi_{s+1})}\cdots\frac{(\xi - \xi_S)}{(\xi_s - \xi_S)}. \tag{8}$$

It is common to employ quadratic Lagrangian polynomials in BEM simulations for acoustic problems, having 3 basis functions per element. In the current work however, higher order functions are studied, ranging from 3-12 basis functions per element, shown in Fig. 1.

4
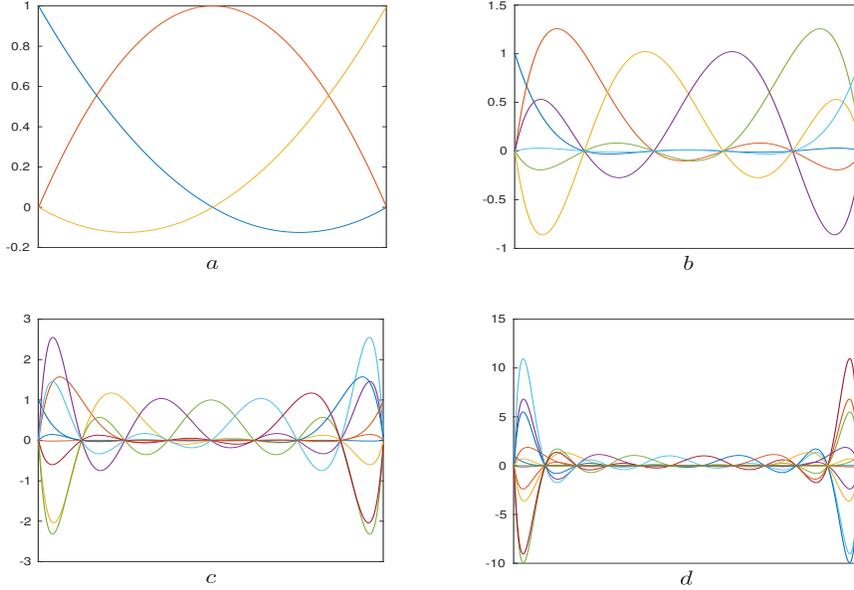
Figure 1: Lagrangian basis functions with a, b, c and d showing $S = 3, 6, 9$ and 12 respectively.

2.2.2 NURBS.

The second basis studied in this paper is a NURBS basis, which describes ϕ as follows.

$$\phi = \sum_{s=0}^{S-1} \Psi_{p,s}^{B}(\xi)\phi_s^e, \tag{9}$$

where

$$\Psi_{p,s}^{B}(\xi) := \frac{N_{p,s}(\xi)w_s}{\sum_{i=0}^{S} N_{i,p}(\xi)w_s} \tag{10}$$

and w_s are a set of weights, $N_{p,s}$ are pth-degree B-spline basis functions, which can be represented for $p > 0$

$$N_{p,s}(\xi) = \frac{\xi - \xi_s}{\xi_{s+p} - \xi_s} N_{p-1,s}(\xi) + \frac{\xi_{s+p+1} - \xi}{\xi_{s+p+1} - \xi_{s+1}} N_{p-1,s+1}(\xi), \tag{11}$$

and for $p = 0$

$$N_{0,s}(\xi) = \begin{cases} 1, & \text{if } \xi_s \leq \xi \leq \xi_{s+1} \\ 0, & \text{otherwise} \end{cases} \tag{12}$$

In line with the Lagrangian basis, we consider 3-12 NURBS basis functions per element, and illustrate in Fig. 2 the case for $w_s = 1, s = 1, ..., S$, for which the NURBS basis reverts to the B-spline basis.

2.2.3 Plane waves.

The third and final basis that is employed in this paper is the plane wave enriched basis of PUBEM. Here, a set of quadratic Langrangian shape functions are multiplied by a linear combination of plane
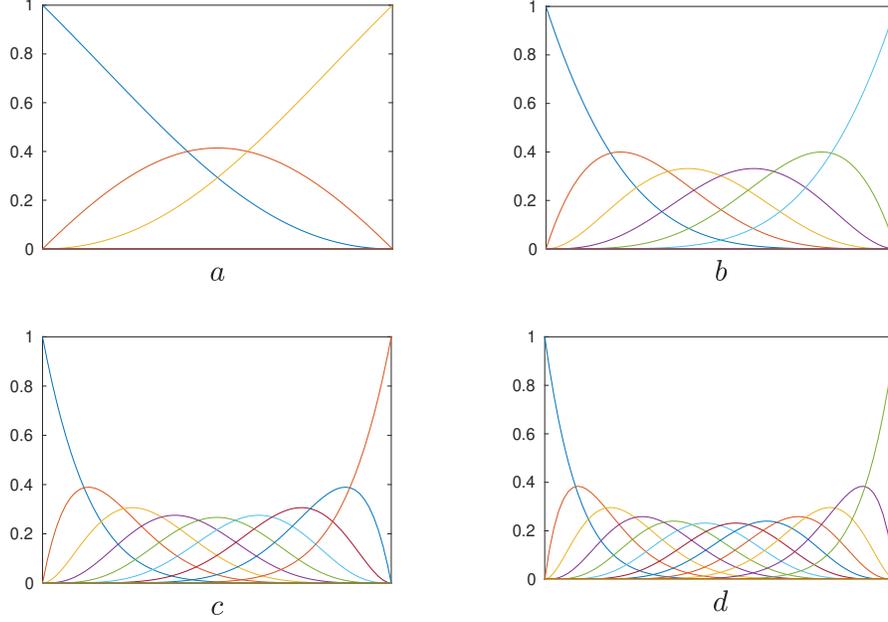
Figure 2: NURBS basis functions with all weights $w_s = 1$; a, b, c and d show $S = 3, 6, 9$ and 12 respectively.

waves propagating in different directions to form the basis functions, as follows.

$$\phi = \sum_{s=1}^{S} \sum_{m=1}^{M} \Psi_s^L(\xi) A_{sm} \mathrm{e}^{ik\mathbf{d}_{sm}\cdot\mathbf{q}}, \tag{13}$$

$$\mathbf{d}_{sm} = (\cos\theta_{sm}, \sin\theta_{sm}), \quad \theta_{sm} = \frac{2\pi(m-1)}{M} \tag{14}$$

M represents the number of plane waves per node, $i = \sqrt{-1}$ and $\mathbf{d}_{sm}$ are the unit direction vectors of propagation of the plane waves. The modified version of (5) is as follows,

$$c(\mathbf{p})\phi(\mathbf{p}) + \sum_{e=1}^{E} \sum_{s=1}^{S} \sum_{m=1}^{M} \int_{-1}^{1} \left[\frac{\partial G(\mathbf{p},\mathbf{q})}{\partial\mathbf{n}} - \alpha G(\mathbf{p},\mathbf{q}) \right] \Psi_s(\xi) e^{ik\mathbf{d}_{sm}\cdot\mathbf{q}} J^e d\xi A_{sm}^e = \int_{\Gamma} G(\mathbf{p},\mathbf{q}) \beta d\Gamma_{\mathbf{q}} + \phi^{inc}(\mathbf{p}), \tag{15}$$

the solution of which produces a set of unknown amplitudes A_{sm} from which the acoustic potential ϕ can be recovered, according to (13).

Before moving on to testing, two aspects relating to implementation are noted here. In PUBEM taking $M > 1$ results in a requirement to collocate at non-nodal locations, meaning that interpolation is required, for example, to apportion the jump terms between the different terms in the matrix row that multiply the non-zero basis functions at the collocation point. Secondly, for exterior problems both BEM and PUBEM can suffer from non-uniqueness of the solution at frequencies corresponding to eigenfrequencies of the associated interior problem. In order to remedy this we adopt in the current work the Combined Helmholtz Integral Equation Formulation (CHIEF) [38] which involves collocating inside the scattering object. This is commonly used in the engineering literature; the resulting system of equations is over-determined and requires an appropriate solver, but is faster and

simpler than the Burton and Miller approach [39] commonly adopted in the mathematics literature
to ensure uniqueness of solution.

3 Numerical testing

3.1 Implementation

In this section high-order NURBS and Lagrange polynomial bases are compared with PUBEM, using an L^2 relative error norm defined as

$$\eta(\phi; \Gamma_\eta) = \frac{||\phi - \phi_{ref}||_{L_2(\Gamma_\eta)}}{||\phi_{ref}||_{L_2(\Gamma_\eta)}}, \tag{16}$$

where ϕ_{ref} is a reference solution and the L^2 norm is taken over a contour Γ_η that will be defined on each usage. Computational efficiency will be presented in terms of the number of degrees of freedom per wavelength, a quantity we denote τ. The condition number, κ, of each resulting system of equations is also observed. Three test cases are considered: scattering by a single cylinder, scattering by multiple cylinders and a plane wave propagating along the length of a duct, all of which have analytical solutions. For the exterior scattering problems, the cylindrical obstacles are assumed to be perfectly reflecting or 'sound-hard', and for the duct the relevant boundary conditions will be presented. Numerical integration is performed using a sub-divided Gauss-Legendre quadrature scheme with a sufficient number of integration points to ensure that the integration error is negligible. A range of discretisations and wave numbers are tested, with an additional pollution study for the duct case. The number of degrees of freedom used is denoted N_d. All codes are implemented in MATLAB.

3.2 Scattering by a cylinder

Scattering by a sound-hard cylinder (i.e. a circular obstacle in $2D$) in an infinite domain is a benchmark problem having an analytical solution [40], wherein the scattered potential at a point $\bar{\mathbf{p}}$ can be represented by a series solution comprised of Bessel functions, as follows.

$$\phi_{ref}(\bar{\mathbf{p}}) = \frac{J_0'(ka)}{H_0'(ka)} H_0(kr) - 2 \sum_{n=1}^{\infty} i^n \frac{J_n'(ka)}{H_n'(ka)} H_n(kr) \cos(n\theta), \quad \bar{\mathbf{p}} \in \Omega_f \tag{17}$$

To represent this example using BEM, a sound-hard Neumann boundary condition is applied on Γ, defined by

$$\frac{\partial \phi(\mathbf{q})}{\partial \mathbf{n}} = 0, \quad \mathbf{q} \in \Gamma. \tag{18}$$

This reduces (5) to

$$c(\mathbf{p})\phi(\mathbf{p}) + \sum_{e=1}^{E} \sum_{s=1}^{S} \int_{-1}^{1} \frac{\partial G(\mathbf{p}, \mathbf{q})}{\partial \mathbf{n}} \Psi_s(\xi) J^e d\xi \phi_s^e = \phi^{inc}(\mathbf{p}) \tag{19}$$

We consider the case of the unit cylinder being impinged by a plane wave travelling in the positive x-direction. The total potential for this example for the case $k = 2\pi$ is shown in Fig. 3. η is evaluated over the circular contour $\Gamma_\eta = \{(x, y) : x = 2\cos\theta, y = 2\sin\theta, \theta \in (0, 2\pi)\}$. For the Lagrange polynomial basis and the NURBS basis we consider four orders $2, 5, 8$ and 11 (as shown in Fig. 1 and Fig. 2). For the PUBEM basis, a fixed number of elements, $E = 4$ is used, increasing N_d by incrementing the number plane waves per node, M.

7
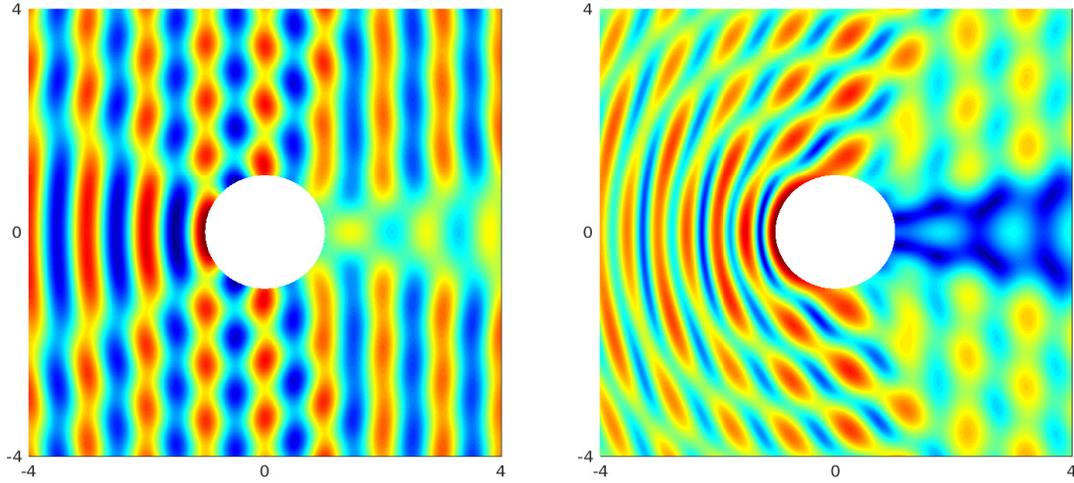
Figure 3: (left) Real part of the total potential, (right) absolute value of total potential, for scattering by a unit cylinder, $k = 2\pi$.
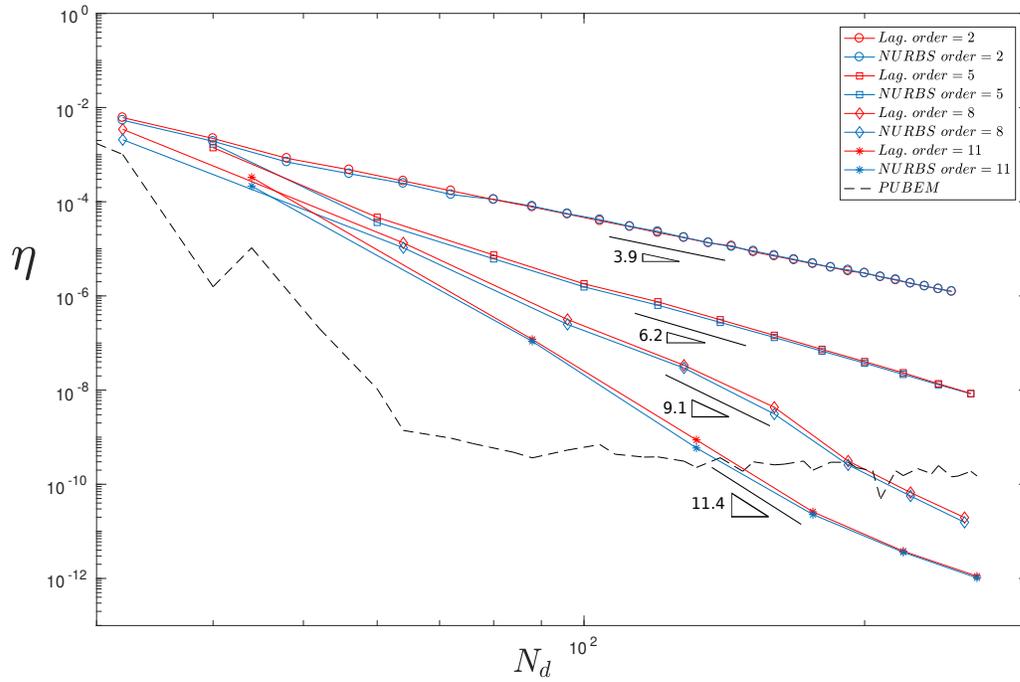
Figure 4: L^2 relative error η vs. N_d for scattering by a unit cylinder, $k = 2\pi$.

Firstly, the wavenumber is fixed at $k = 2\pi$ but N_d is increased to ≈ 250, which corresponds to $\tau \approx 40$. This far exceeds the requirement to achieve 'engineering accuracy' with any of the basis functions that are being tested, but it offers insight into the broader numerical behaviour. The results can be seen in Fig. 4, which shows a clear benefit in computational efficiency from using higher order functions. These results are somewhat expected as in [28] we see an increase in accuracy as a result of increasing the order of a NURBS basis from 2-3, for elasticity problems. It is evident that the Lagrange and NURBS bases offer similar numerical performance, and that the NURBS basis does not offer the clearer improvement that has been seen in other, predominantly low-order, IGABEM applications. Though, 3rd order NURBS and Lagrange shape functions are shown to converge at a similar rate for acoustic scattering by a torus in [29]. We consider the following explanation. IGABEM can be expected to give improvements over the classical piecewise polynomial basis for two reasons: (i) the exact geometric description, and (ii) the smoother, non-negative basis. As long as the geometric error produced by the Lagrange basis functions is small in comparison with the wavelength, the implications on the solution error will be limited. Once the Lagrange models in this study are sufficiently refined to observe the heuristic on the required τ, the geometric description is certainly of sub-wavelength accuracy, so the difference we are seeing in the errors is likely to reduce to the effect of the improved smoothness and non-negativity of the NURBS basis. It can be seen that this effect is a mild one, so that the errors produced by high order Lagrange and NURBS bases are rather similar. For simple geometries, it would also be possible to use a more compact geometric description with a lower order NURBS than that used to approximate the acoustic potential solution, in a similar way to the use of the classical idea of sub-parametric finite elements.

PUBEM is seen to quickly achieve a higher level of accuracy, but is eventually overtaken by the higher order NURBS and Lagrange bases with the increased severity of ill-conditioning in the PUBEM linear system at large τ [16]. In order to illustrate this, the condition number κ is shown for the Lagrange and NURBS systems in Fig. 5, which indicates that whilst increasing the order of basis functions employed does increase κ, increasing N_d has no detrimental impact on the condition number. Contrary to this, Fig. 6 shows a direct comparison between κ, N_d and η for the PUBEM case and it is evident that as the degrees of freedom increase, so does the condition number, and the limitations of the solver restrict the accuracy of the solution. Notwithstanding this comment, it is clear that, as long as a suitable solver is chosen that can deal with such ill-conditioned matrices, the most accurate PUBEM solutions are to be found from the most poorly conditioned systems because these benefit from the most enriched approximation space.

PUBEM is designed as a method specifically aimed at the mid-high frequency range. We are testing it here for problems with lower k to investigate its performance against Lagrange and NURBS bases. For this reason, another comparison is made for the single cylinder case, in which N_d is fixed, but k varies. It is not possible to force the number of degrees of freedom used for each basis to equal one another, but for each discretisation $N_d \in [220, 224]$; the results are displayed in Fig. 7. The results show that, as expected, PUBEM outperforms the other methods at high frequency, but importantly it is evident that the high-order methods function optimally at large τ (i.e. at small k when N_d is fixed) whereas the converse is true for PUBEM.

3.3 Scattering by three cylinders

The second example considered is the scattering of an incident plane wave by 3 sound-hard circular cylinders in an infinite domain. The problem has an analytical solution [41], wherein the scattered potential ϕ_{ref} for a set of N cylinders can be represented on the boundary of the vth cylinder by a series solution comprised of Hankel functions,

$$\phi_{ref}(a_v, \theta_v) = -\frac{2i}{\pi k a_v} \sum_{n=-\infty}^{\infty} \frac{A_n^v}{H_n'(k a_v)} e^{in\theta_v}, \tag{20}$$

9
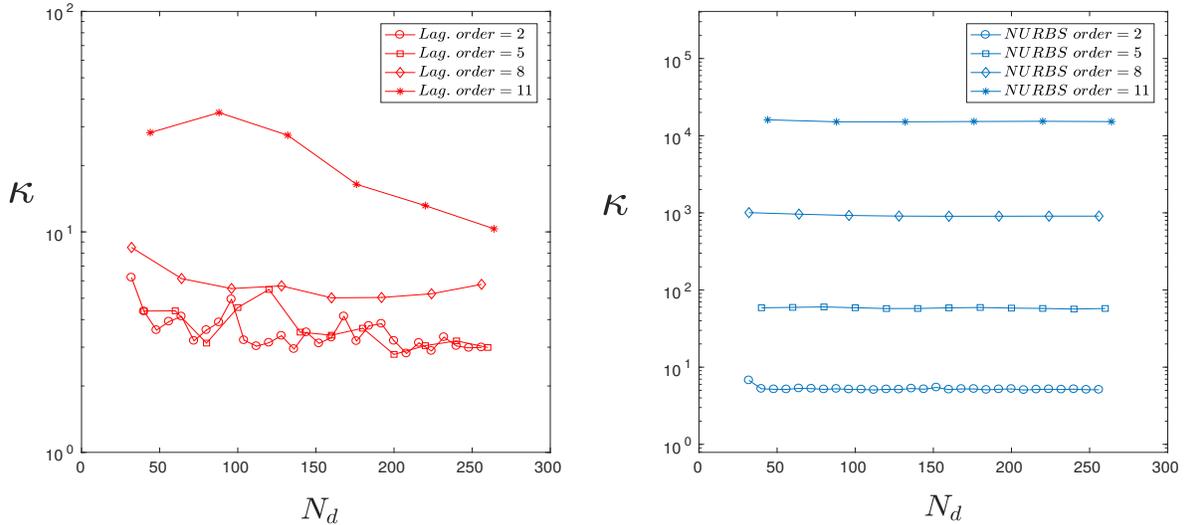
Figure 5: (Left) Condition number κ vs. N_d for Lagrange basis, (Right) Condition number κ vs. N_d for NURBS basis, for scattering by a unit cylinder, $k = 2\pi$.

where a_v is the radius of the vth cylinder, θ_v is the angle from the positive x-axis of the vth cylinder to the point of evaluation and H_n is a Hankel function of the first kind and order n. The infinite series can be truncated to a finite number of terms, with A_n^v obtained according to [41]. We define the boundary of each cylinder as Γ_1, Γ_2 and Γ_3 and evaluate the error norm η over their union so that $\Gamma_\eta = \bigcup_{v=1}^{v=3} \Gamma_v$.

We consider the case of three unit cylinders located at a radius of 3 from the origin $(0,0)$ with centres at angles of $0, \frac{2\pi}{3}$ and $\frac{4\pi}{3}$, being impinged by a plane wave travelling in the positive x-direction. The total potential for this example with $k = 4\pi$ is shown in Fig. 8. It is evident that with the inclusion of reflections, the solution is more complicated than that of the single cylinder.

The same selection of basis functions and discretisations employed for the single cylinder example, are applied to each cylinder in this example. As with the single cylinder example, we fix the wavenumber, for this case at $k = 4\pi$, and vary the degrees of freedom per circle up to ≈ 250. The results in Fig. 9 display very similar behaviour to those obtained for the single cylinder. There is a clear benefit in using high-order basis functions and the Lagrange results are in close agreement with the NURBS results. There is also very similar behaviour with the PUBEM results, reaching a high level of accuracy quickly, before gradually being overtaken by the high-order NURBS and Lagrange functions, due to conditioning limitations. This happens slightly later (at $N_d \approx 210$) than for the single cylinder case ($N_d \approx 140$), which the authors attribute to the increase in k, because this produces a τ range that is more favourable for PUBEM. The respective condition numbers of the resulting systems of equations are shown in Fig. 10 for the Lagrange and NURBS basis, with the PUBEM condition number in Fig. 11. It is clear that the behaviour is similar to the previous example again, as the lowest condition numbers are seen in the Lagrange basis, with a slight increase associated with the NURBS basis and a substantial increase for PUBEM. It is worth noting that using PUBEM offers an improvement in η of 4-5 orders of magnitude over the conventional quadratic Lagrange polynomial basis for much of the N_d range.
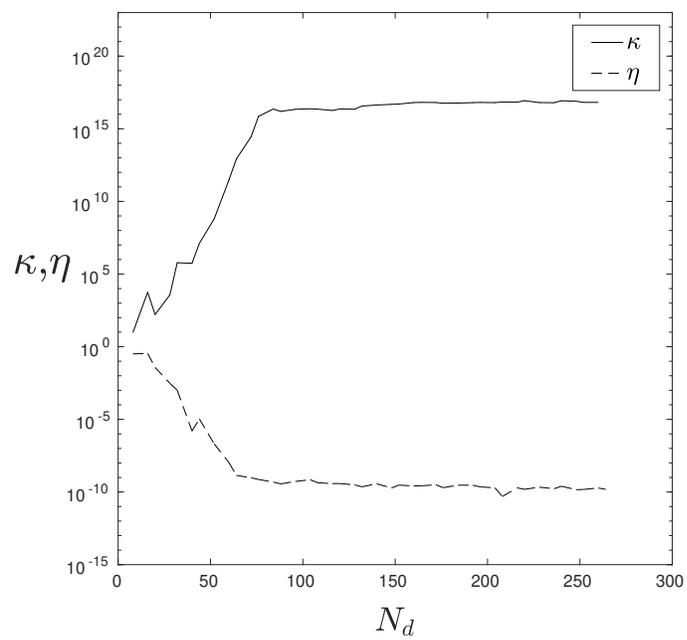
Figure 6: PUBEM L^2 relative error η and condition number κ for scattering by a unit cylinder, $k = 2\pi$.
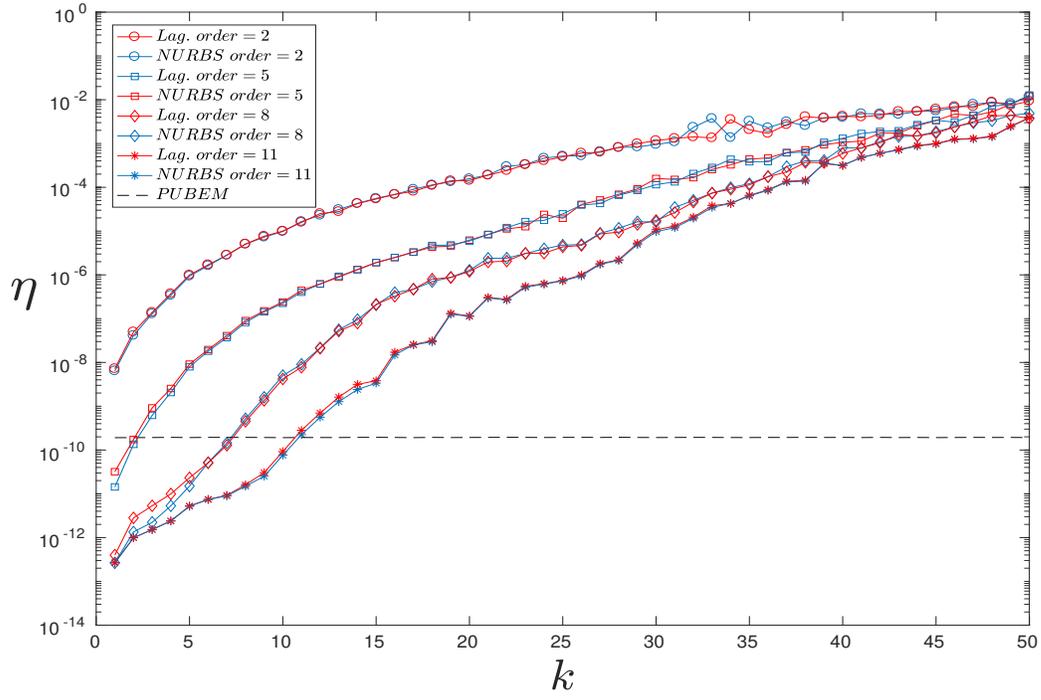
Figure 7: L^2 relative error η for scattering by a unit cylinder, with $N_d \in$ 220-224.
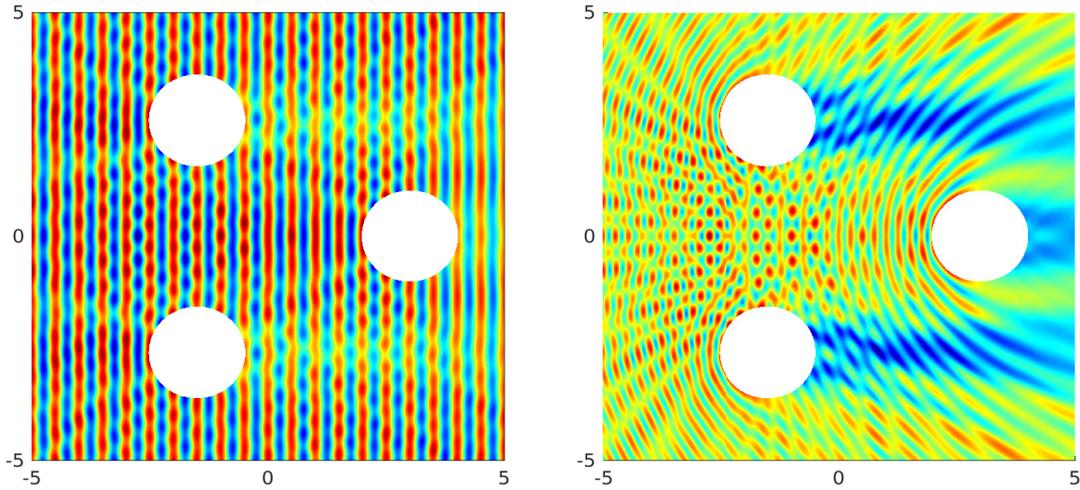
Figure 8: (left) Real part of the total potential, (right) absolute value of total potential, for scattering by three unit cylinders, $k = 4\pi$.
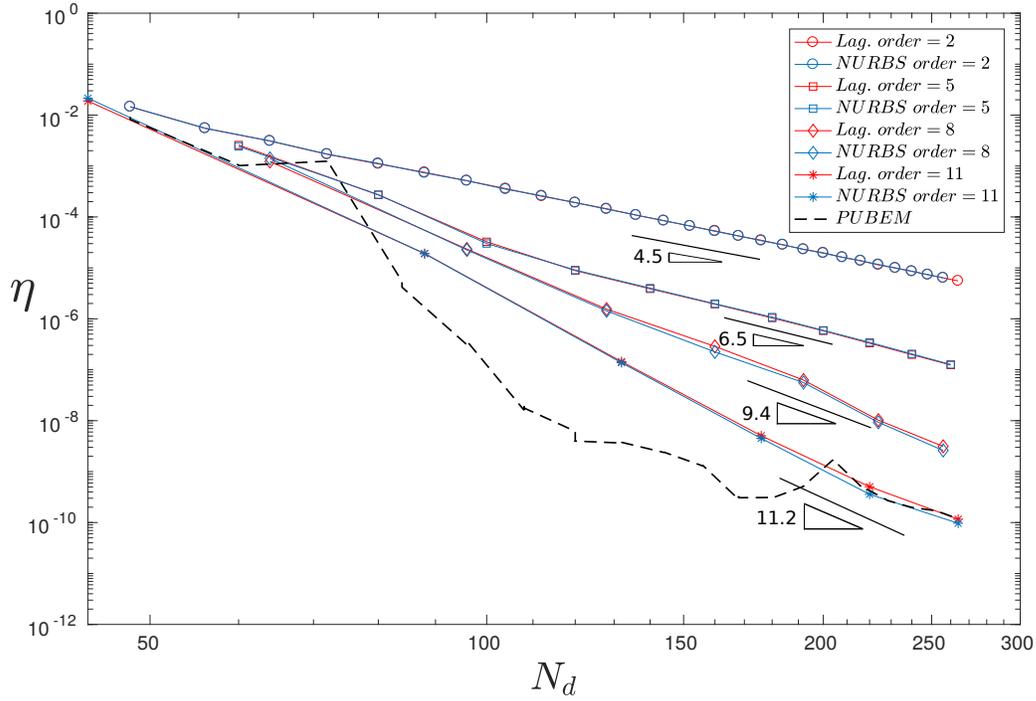
Figure 9: L^2 relative error η vs N_d (per cylinder) for scattering by three unit cylinders, $k = 4\pi$.
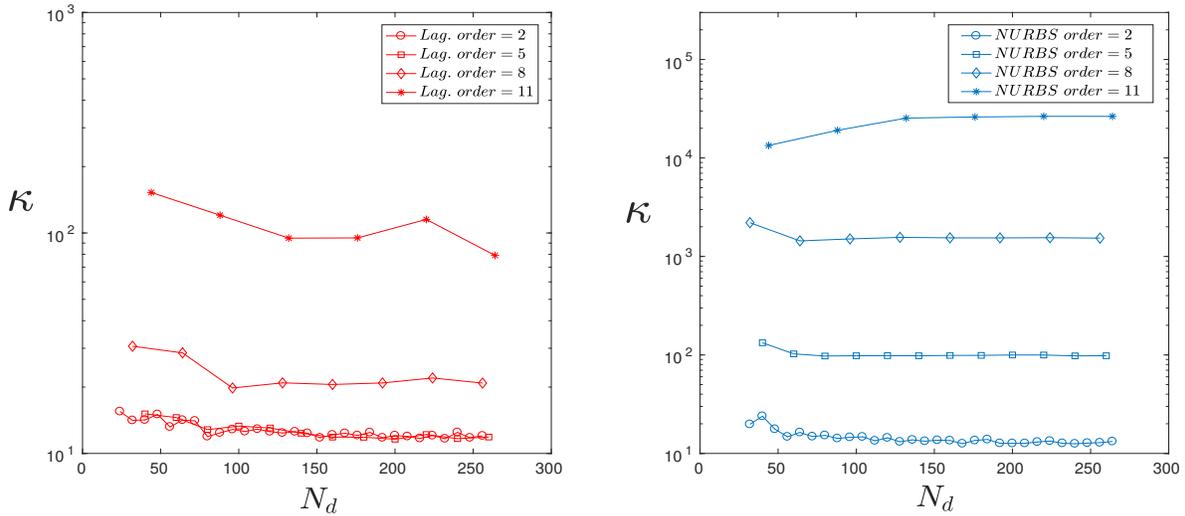
Figure 10: (Left) Condition number κ vs. N_d for Lagrange basis, (Right) Condition number κ vs. N_d for NURBS basis, for scattering by three unit cylinders, $k = 4\pi$.

13
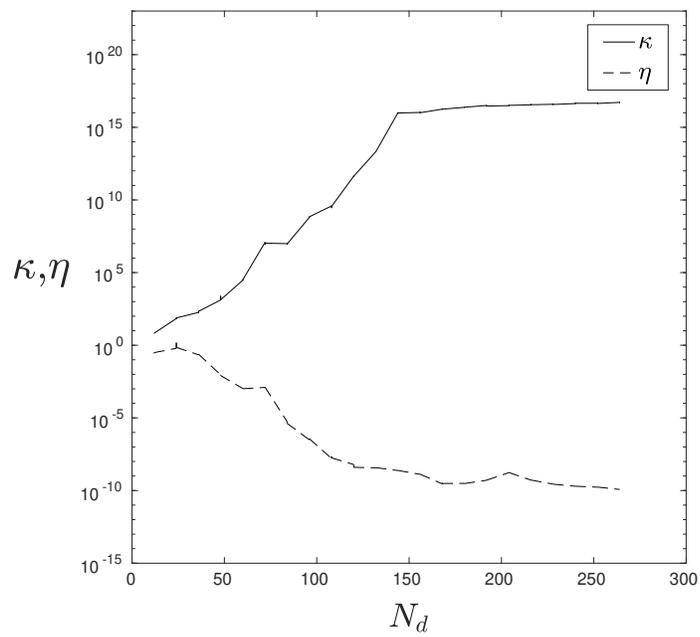
Figure 11: PUBEM L^2 relative error η and condition number κ for scattering by three unit cylinders, $k = 4\pi$.

3.4 Plane wave propagating along the length of a duct

The third example is a plane wave propagating along the length of a duct, which is in essence a $1D$ problem, but is being analysed here in $2D$. We consider the analytical case wherein the potential at a point $\bar{\mathbf{p}}$ is given by

$$\phi_{ref}(\bar{\mathbf{p}}) = e^{ikx(\bar{\mathbf{p}})}, \quad \bar{\mathbf{p}} \in \Omega_f. \tag{21}$$
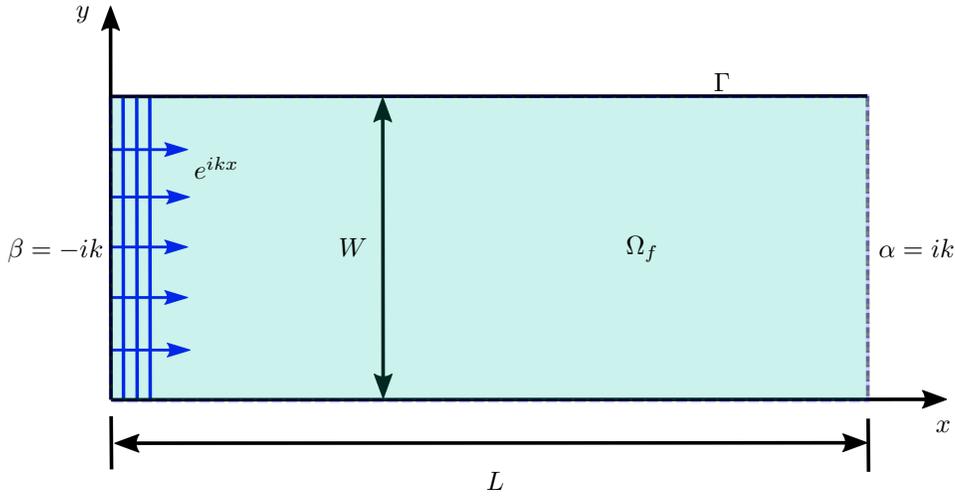
Figure 12: Duct boundary conditions and domain.

We consider this as an acoustic cavity problem with Robin boundary conditions $\alpha = 0, \beta = -ik$ prescribed on the left hand side of the duct, and $\alpha = ik, \beta = 0$ on the right hand side; these can be seen along with relevant dimensions in Fig. 12. Along the horizontal boundaries we prescribe $\alpha = 0$ and $\beta = 0$, corresponding to the 'sound-hard' condition. We evaluate the error norm η over the line $\Gamma_\eta = \{(x,y) : x \in (0,L), y = W/2\}$. Results from a test case in a short duct of dimensions $L = 1$, $W = 1$, with $k = 4\pi$, are displayed in Fig. 13, and it is evident that the error η follows a similar pattern to that in the previous examples. Increasing the order of basis functions employed causes a reduction in error, with Lagrange polynomials and NURBS offering similar performance.

Before discussing the PUBEM results, details of the PUBEM discretisation should be outlined. To generate the plots of error norm η for the Lagrange and NURBS schemes in Fig. 13, the process is straightforward; first select the order of basis to be employed, then increase the number of elements to give the required total number of degrees of freedom. For example, in the first two examples of exterior scattering from cylinders, a coarse discretisation of 4 elements per cylinder was used, with M chosen to provide the required number of degrees of freedom, N_d. In PUBEM there are two options, one can increase the total number of elements, E (i.e. h-refinement), or increase the number of plane waves M included per node (a process akin to p-refinement, and sometimes called Q-refinement). It has been shown that the latter is favourable [17], until τ becomes sufficiently large to cause severe ill-conditioning, at which point an increase in the number of elements, E, with an associated reduction in the number of plane waves M, becomes the favourable option. This is similar to the hp-refinement schemes commonly found in the finite element literature.

In this problem, the obvious choice is to include the x-direction in the set of plane waves used to form the basis. Clearly, then, the solution to the problem is contained in the approximation space and it would be expected that a solution with very low errors would be obtained. This is indeed

the case, and one can also reduce M to 1 (i.e. including only the x-direction and no other directions in the plane wave basis). This is demonstrated in Table 1, which displays η for a range of ducts of length L up to 200λ for the case $k = 4\pi$, with only a single element used on each side of the duct. It is evident that a high level of accuracy is consistently achieved for this coarsest of meshes, independently of L.

We repeat that this high accuracy for such a small number of degrees of freedom comes as no surprise, since the exact solution is contained in the approximation space. However, it is more interesting to investigate the performance of PUBEM where $M > 1$ and the x-direction is *not* contained in the basis. It is well known that a linear combination of (a sufficient number of) plane waves can reproduce any solution of the Helmholtz equation, and here we explore the behaviour of PUBEM with this multiple wave expansion in approximating the plane wave propagating through the duct. It is this set of plane wave directions (not including $\theta = 0$) that has been used to produce the PUBEM results in Fig. 13. Clearly it remains possible to recover the acoustic potential with high accuracy.
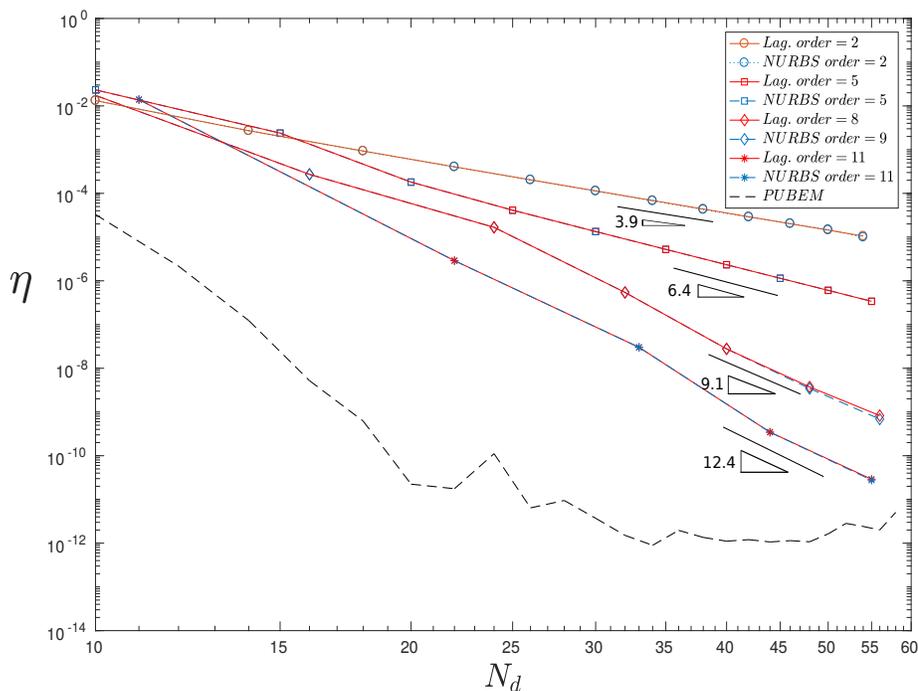
Figure 13: L^2 error η vs. N_d per side for a travelling wave in a duct, $k = 4\pi$.

L/λ	2	20	100	200
τ	1	0.1	0.02	0.01
η	$3.0996e-13$	$3.5676e-13$	$3.5802e-13$	$3.4503e-13$

Table 1: Relative error η with $M = 1$ using only a single element per side, $k = 4\pi$.

16
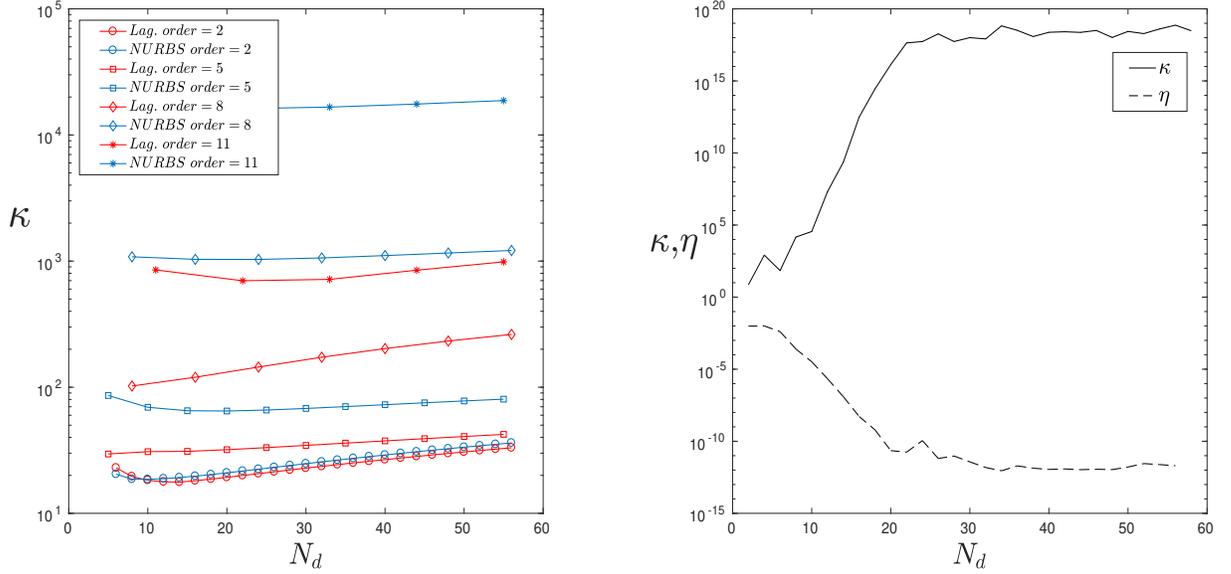
Figure 14: (left) Condition number κ for the Lagrange and NURBS basis, (right) Condition number κ and L^2 error η for the plane wave basis, for a travelling wave in a duct, $k = 4\pi$.

3.4.1 Pollution error in the duct.

Pollution error is a commonly studied numerical aspect of FEM schemes for Helmholtz problems [1]. But it has only recently been investigated for the BEM by Marburg [35], who used piecewise constant, linear and quadratic basis functions in a BEM approximation of propagation of a plane wave along a long, slender, air-filled duct. A pollution effect was observed in this BEM study. In this section, we explore the same duct, with the same number of degrees of freedom per side as the finest of Marburg's discretisations, but using high-order and plane wave enriched basis functions. The dimensions of this example are $W = 0.2$ m and $L = 54.4$ m, with the speed of sound in air taken to be 340 m/s and a frequency of 750 Hz.

To produce the results, 1632 degrees of freedom are included along each of the long sides of the duct, and a local absolute error $\eta_1 = |\phi - \phi_{ref}|$, is computed over Γ_η. From observing η_1 in Fig. 15 it is clear that both the Lagrange and NURBS bases are subject to a pollution effect manifested in degradation in accuracy with increasing coordinate x. Increasing the order of basis employed does reduce the overall error, but the error is seen to increase as a function of x. Again, the results of the Lagrange and NURBS bases produce very similar results (the conditioning is benign in both cases, and the condition numbers for this example are shown in Table 2). The PUBEM discretisations employed are $M = 1, 8, 10$ and 12, with the corresponding number of elements, E, to provide the appropriate number of degrees of freedom per side. For the $M = 8, 10$ and 12 discretisations the plane wave directions are equispaced, but the x-direction is explicitly excluded from the basis, whereas for the $M = 1$ case, it is the only direction included in the basis. Fig 16 displays the variation in error η_1 with position in the duct. For the case $M = 1$ the errors are consistently very small, and there is no evidence of any meaningful pollution error. For $M = 8, 10, 12$ the errors are highly oscillatory in x, which may perhaps be expected for errors in the range 10^{-9} to 10^{-11}, but a small underlying positive gradient is visible that suggests there is a mild pollution effect when

Lagrange		NURBS		PUBEM	
Order	κ	Order	κ	M	κ
2	50.3	2	51.5	1	49.6
5	47.8	5	72.8	8	$1.9e + 18$
8	90.6	8	1137.3	10	$1.3e + 19$
11	1341.6	11	1972.4	12	$3.6e + 18$

Table 2: Condition number κ for the duct with $L = 54.4m$, $W = 0.2m$ and $f = 750Hz$
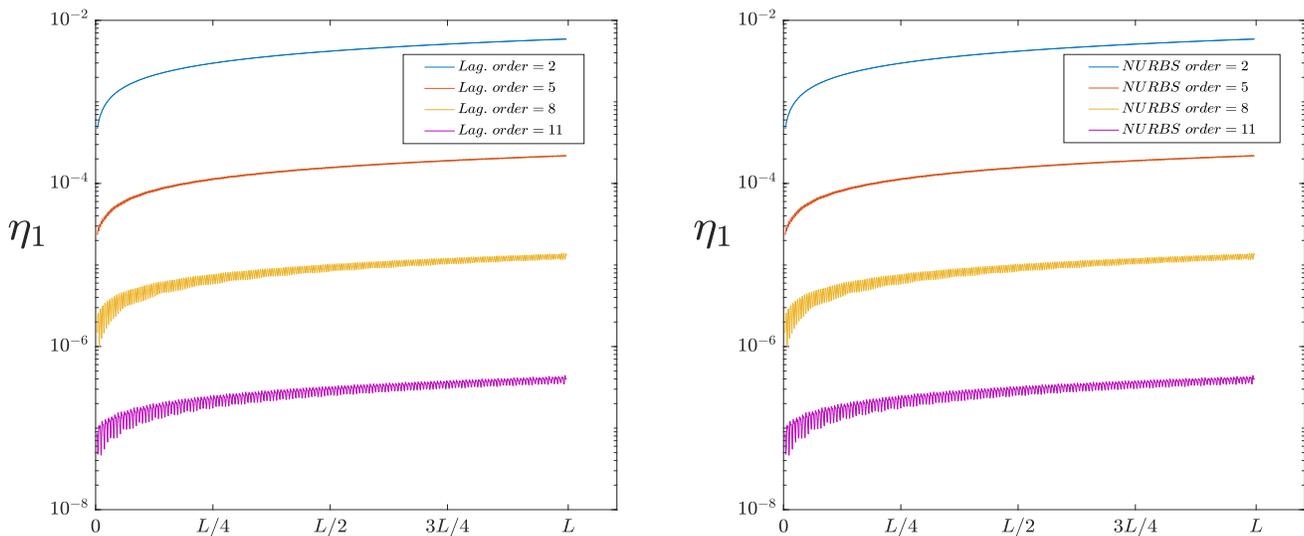
Figure 15: (left) Local error η_1 for the Lagrange basis, (right) Local error η_1 for the NURBS basis for a travelling wave in a duct having $L = 54.4$, $f = 750Hz$, and including 1632 degrees of freedom on each long side.

using a plane wave basis. These results for pollution errors in the PUBEM are consistent with the observations of Gittelson for the plane-wave enriched Discontinuous Galerkin (PWDG) method [36].

4 Conclusions

Numerical performance of high-order NURBS and Lagrange polynomial bases has been compared with the plane wave basis of PUBEM for three benchmark problems. Results show a marked improvement in accuracy from increasing the order of NURBS and Lagrange polynomial bases, with a reduction in error of up to 6 orders of magnitude. The resulting condition number of the system of equations increases along with the order, but for the examples studied by the authors (up to 11th order functions per element), both systems are well conditioned and the accuracy of the solution is not adversely affected. The NURBS and Lagrange basis sets provide very similar numerical solutions in the relative L^2 error norm, with NURBS performing slightly the better of the two. The PUBEM has been shown to consistently outperform the lower order bases, but for large τ the 11th order

18
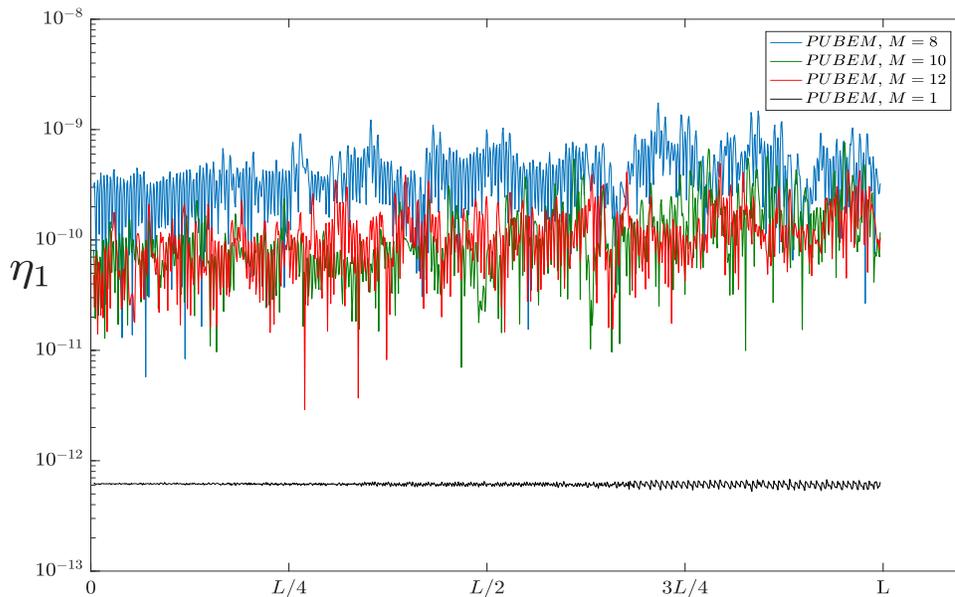
Figure 16: Local error η_1 for the PUBEM basis for a travelling wave in a duct having $L = 54.4$, $f = 750Hz$, and including 1632 degrees of freedom on each long side.

Lagrange and NURBS bases generate better conditioned linear systems and can achieve greater accuracy. Additionally, the pollution error in BEM has been observed in an example of a travelling wave in a long duct, even whilst employing high-order basis functions, or a plane wave basis. The overall error in the duct can reduced by increasing the order of the basis functions, or by enriching it, but a pollution error will still develop for waves propagating over a long distance.

References

[1] Ihlenburg, F. and Babuška, I., 1997. Finite element solution of the Helmholtz equation with high wave number part II: the hp version of the FEM. SIAM Journal on Numerical Analysis, 34(1), pp.315-358.

[2] Babuška, I., Ihlenburg, F., Paik, E.T. and Sauter, S.A., 1995. A generalized finite element method for solving the Helmholtz equation in two dimensions with minimal pollution. Computer methods in applied mechanics and engineering, 128(3-4), pp.325-359.

[3] Petersen, S., Dreyer, D. and von Estorff, O., 2006. Assessment of finite and spectral element shape functions for efficient iterative simulations of interior acoustics. Computer methods in applied mechanics and engineering, 195(44-47), pp.6463-6478.

[4] Bériot, H., Prinn, A. and Gabard, G., 2016. Efficient implementation of highorder finite elements for Helmholtz problems. International Journal for Numerical Methods in Engineering, 106(3), pp.213-240.

[5] El Kacimi, A., Laghrouche, O., Mohamed, M.S. and Trevelyan, J., 2018. Bernstein-Bézier based finite elements for efficient solution of short wave problems. Computer Methods in Applied Mechanics and Engineering.

[6] Babuška, I. and Melenk, J.M., 1997. The Partition of Unity Method. International Journal for Numerical Methods in Engineering, 40(4), pp.727-758.

[7] Melenk, J.M. and Babuška, I., 1996. The partition of unity finite element method: basic theory and applications. In Research Report/Seminar fr Angewandte Mathematik (Vol. 1996, No. 01). Eidgenssische Technische Hochschule, Seminar fr Angewandte Mathematik.

[8] Laghrouche, O., Bettess, P. and Astley, R.J., 2002. Modelling of short wave diffraction problems using approximating systems of plane waves. International Journal for Numerical Methods in Engineering, 54(10), pp.1501-1533.

[9] Laghrouche, O., Bettess, P., Perrey-Debain, E. and Trevelyan, J., 2005. Wave interpolation finite elements for Helmholtz problems with jumps in the wave speed. Computer Methods in Applied Mechanics and Engineering, 194(2-5), pp.367-381.

[10] Ladevéze, P., Arnaud, L., Rouch, P. and Blanzé, C., 2001. The variational theory of complex rays for the calculation of medium-frequency vibrations. Engineering Computations, 18(1/2), pp.193-214.

[11] Hiptmair, R., Moiola, A. and Perugia, I., 2011. Plane wave discontinuous Galerkin methods for the 2D Helmholtz equation: analysis of the p-version. SIAM Journal on Numerical Analysis, 49, pp.264-284.

[12] Gabard, G., 2007. Discontinuous Galerkin methods with plane waves for time-harmonic problems. Journal of Computational Physics, 225, pp.1961-1984.

[13] Farhat, C., Harari, I. and Franca, L.P., 2001. The discontinuous enrichment method. Computer Methods in Applied Mechanics and Engineering, 190(48), pp.6455-6479.

[14] Cessenat, O. and Despres, B., 1998. Application of an ultra weak variational formulation of elliptic PDEs to the two-dimensional Helmholtz problem. SIAM Journal on Numerical Analysis, 35(1), pp.255-299.

[15] Colton, D. and Kress, R. 1993 , Integral Equation Methods in Scattering Theory, Springer.

[16] Perrey-Debain, E., Trevelyan, J. and Bettess, P., 2004, 2002. New special wave boundary elements for short wave problems. Communications in Numerical Methods in Engineering, 18(4), pp.259-268.

[17] Perrey-Debain, E., Trevelyan, J. and Bettess, P., 2004. Wave boundary elements:a theoretical overview presenting applications in scattering of short waves, Eng. Anal Bound. Elem., 28: 131–141.

[18] Perrey-Debain, E., Laghrouche, O., Bettess, P. and Trevelyan, J., 2004. Plane-wave basis finite elements and boundary elements for three-dimensional wave scattering. Philosophical Transactions of the Royal Society of London A: Mathematical, Physical and Engineering Sciences, 362(1816), pp.561-577.

[19] Chandler-Wilde, S.N. and Langdon, S., 2007. A Galerkin boundary element method for high frequency scattering by convex polygons. SIAM Journal on Numerical Analysis, 45(2), pp.610-640.

[20] Groth, S.P., Hewett, D.P. and Langdon, S., 2015. Hybrid numericalasymptotic approximation for high-frequency scattering by penetrable convex polygons. IMA Journal of Applied Mathematics, 80(2), pp.324-353.

[21] Barnett, A.H. and Betcke, T., 2008. Stability and convergence of the method of fundamental solutions for Helmholtz problems on analytic domains. Journal of Computational Physics, 227, pp.7003-7026.

[22] Hughes, T. J. R., Cottrell, J. A. and Bazilevs, Y., 2005. Isogeometric analysis: CAD, finite elements, NURBS, exact geometry and mesh refinement. Computer Methods in Applied Mechanics and Engineering, 194, pp.4135-4195.

[23] Bazilevs, Y., Calo, V.M., Hughes, T.J. and Zhang, Y., 2008. Isogeometric fluid-structure interaction: theory, algorithms, and computations. Computational mechanics, 43(1), pp.3-37.

[24] Buffa, A., Sangalli, G. and Vázquez, R., 2010. Isogeometric analysis in electromagnetics: B-splines approximation. Computer Methods in Applied Mechanics and Engineering, 199(17-20), pp.1143-1152.

[25] Cottrell, J.A., Reali, A., Bazilevs, Y. and Hughes, T.J., 2006. Isogeometric analysis of structural vibrations. Computer methods in applied mechanics and engineering, 195(41-43), pp.5257-5296.

[26] Politis, C., Ginnis, A.I., Kaklis, P.D., Belibassakis, K. and Feurer, C., 2009, October. An isogeometric BEM for exterior potential-flow problems in the plane. In 2009 SIAM/ACM Joint Conference on Geometric and Physical Modeling (pp. 349-354).

[27] Li, K. and Qian, X., 2011. Isogeometric analysis and shape optimization via boundary integral. Computer-Aided Design, 43(11), pp.1427-1437.

[28] Simpson, R.N., Bordas, S.P., Trevelyan, J. and Rabczuk, T., 2012. A two-dimensional isogeometric boundary element method for elastostatic analysis. Computer Methods in Applied Mechanics and Engineering, 209, pp.87-100.

[29] Simpson, R.N., Scott, M.A., Taus, M., Thomas, D.C. and Lian, H., 2014. Acoustic isogeometric boundary element analysis. Computer Methods in Applied Mechanics and Engineering, 269, pp.265-290.

[30] Peake, M.J., Trevelyan, J. and Coates, G., 2013. Extended isogeometric boundary element method (XIBEM) for two-dimensional Helmholtz problems. Computer Methods in Applied Mechanics and Engineering, 259, pp.93-102.

[31] Peake, M.J., Trevelyan, J. and Coates, G., 2015. Extended isogeometric boundary element method (XIBEM) for three-dimensional medium-wave acoustic scattering problems. Computer Methods in Applied Mechanics and Engineering, 284, pp.762-780.

[32] Lieu, A., Gabard, G. and Bériot, H., 2016. A comparison of high-order polynomial and wave-based methods for Helmholtz problems. Journal of Computational Physics, 321, pp.105-125.

[33] Diwan, G.C. and Mohamed, M.S., 2019. Pollution studies for high order isogeometric analysis and finite element for acoustic problems. Computer Methods in Applied Mechanics and Engineering, 350, pp.701-718.

[34] Khajah, T., Antoine, X. and Bordas, S., 2016. Isogeometric finite element analysis of time-harmonic exterior acoustic scattering problems. arXiv preprint arXiv:1610.01694.

[35] Marburg, S., 2018. A pollution effect in the boundary element method for acoustic problems. Journal of theoretical and computational acoustics, 26(02), p.1850018.

[36] Gittelson, C.J. and Hiptmair, R., 2014. Dispersion analysis of plane wave discontinuous Galerkin methods. International Journal for Numerical Methods in Engineering, 98(5), pp.313-323.

[37] A. A. Becker, 1992. *The boundary element method in engineering: a complete course*, McGraw-Hill, Maidenhead.

[38] Schenck, H.A., 1968. Improved integral formulation for acoustic radiation problems. The journal of the acoustical society of America, 44(1), pp.41-58.

[39] Burton, A.J. and Miller, G.F., 1971. The application of integral equation methods to the numerical solution of some exterior boundary-value problems. Proc. R. Soc. Lond. A, 323(1553), pp.201-210.

[40] Jones, D.S., 1986. *Acoustic and electromagnetic waves*, Oxford/New York, Clarendon Press/Oxford University Press.

[41] Linton, C.M. and Evans, D.V., 1990. The interaction of waves with arrays of vertical circular cylinders. Journal of fluid mechanics, 215, pp.549-569.